# Stable interstitial dopant–vacancy complexes in ZnO

B. Puchala and D. Morgan

*Department of Materials Science and Engineering, University of Wisconsin–Madison, Madison, Wisconsin 53706, USA*

(Received 13 October 2011; published 18 May 2012; corrected 15 February 2013)

Using *ab initio* calculations, we have identified stable group-V dopant-vacancy complexes complexes in ZnO consisting of interstitial dopants surrounded by three $V_{Zn}$ ($D_I$-3$V_{Zn}$ with $D$ = P, As, or Sb). In contradiction with previous reports, our calculations show that the acceptor level of group-V dopant–vacancy complexes is too deep to be the shallow acceptor level identified experimentally as contributing to $p$-type conductivity in ZnO. The interstitial-vacancy complexes we have identified can be generalized to other compositions, dopants, and structures.

DOI: 10.1103/PhysRevB.85.195207 PACS number(s): 61.72.J−, 61.72.Bb, 61.72.uj, 71.55.Gs

ZnO is a potentially important material for optoelectronic devices operating in the blue-to-ultraviolet range, but the lack of reliable, reproducible $p$-type ZnO is limiting its widespread use. There are many reports of $p$-type conductivity in group-V-doped ZnO, which is widely attributed to acceptor complexes consisting of group V dopants substituting on Zn sites ($D_{Zn}$ with $D$ = P, As, or Sb) and Zn vacancies ($V_{Zn}$). Based on theoretical calculations,[1] $D_{Zn}$-2$V_{Zn}$ acceptor complexes (a substitutional dopant on a Zn site complexed with two neighboring vacancies on Zn sites) seem to be a good explanation for measurements of $p$-type conductivity in group-V-doped ZnO. Their presence is supported by a low calculated formation energy and agreement of their calculated transition levels with levels identified in experiments,[2–10] which range from 0.09 to 0.34 eV above the valence-band maximum (VBM). In addition, $D_{Zn}$-2$V_{Zn}$ complexes are consistent with experimental evidence that implanted As and Sb incorporate on Zn sites.[11,12] Furthermore, $p$-type conductivity emerging from these complexes is consistent with the need for O-rich-growth or annealing conditions to create $p$-type samples as these defects are stabilized by high oxygen partial pressures.

However, the lack of efficient ZnO-homojunction-based devices suggests that doping with group V elements has not actually been successful. Experiments have shown that the conductivity type can have a strong spatial dependence related to sample topography,[13] that $p$-type conductivity is associated with increased dislocation density,[8] and that luminescence may be either correlated[14] or anticorrelated[15] with the presence of stacking faults and dislocations. For these reasons, acceptors localized at stacking faults[14] and hole accumulation at interfaces with precipitates[16] have also been proposed as possible causes of the $p$-type measurements rather than $D_{Zn}$-2$V_{Zn}$ acceptor complexes. Here, we provide further evidence that dopant-vacancy complexes do not result in $p$-type conductivity. Using *ab initio* calculations, we have found that complexes consisting of interstitial dopants surrounded by three $V_{Zn}$ ($D_I$-3$V_{Zn}$ complexes) are in fact more stable than $D_{Zn}$-2$V_{Zn}$ complexes and that both are deeper acceptors than those typically identified in experiments. These results suggest that bulk $D_{Zn}$-2$V_{Zn}$ defect clusters do not lead to $p$-type conductivity and provide additional support for the need of an alternative explanation.

For all calculations, we used the VIENNA *AB INITIO* SOFTWARE PACKAGE.[17] We used the generalized gradient approximation (GGA) as parametrized by Perdew, Burke, and Ernzerfhof (PBE)[18] for the exchange-correlation functional. Except where noted, we treated errors in the band gap of ZnO due to inadequate repulsion between Zn 3$d$ and conduction-band levels with the GGA + U correction.[19] We used the value $U$-$J$ = 7.5 eV (Ref. 20) so that the valence-band and Zn 3$d$ energy levels match experiment and self-interaction-corrected calculations. Spin polarization was used for those defects with a net magnetic moment: $V_{Zn}^{0}$, $V_{Zn}^{1-}$, and neutral $D_{Zn}$-2$V_{Zn}$ and $D_I$-3$V_{Zn}$ complexes. We used the projector-augmented-plane-wave (PAW) method, and the plane-wave-energy cutoff was 600 eV. To avoid interactions between neighboring periodic images, the defect calculations were performed in wurtzite-ZnO supercells with 256 atoms ($4 \times 4 \times 4$ unit cells) in the undefected cell. We used Γ-only $k$-point sampling for calculations that involved checking the formation-energy difference between cluster configurations with $V_{Zn}$ at the first-nearest-neighbor (1NN) and at a farther apart positions. All other GGA and GGA + U calculations of clusters used a Γ-point-centered $2 \times 2 \times 2$ Monkhorst-Pack $k$-point mesh.[21] The supercell-lattice vectors and all atomic positions were allowed to fully relax.

The formation energy of defects is defined as[22]

$$E_f = E^{\text{def}} - E^{\text{undef}} - \sum_i \Delta n_i \mu_i + \Delta q \mu_F, \qquad (1)$$

where $E_{\text{def}}$ and $E_{\text{undef}}$ are the total energy of the defected and undefected supercells, respectively; $\Delta n_i$ is the number of species $i$ added to the undefected material from the reservoir (i.e., +1 for an interstitial and −1 for a vacancy); $\mu_i$ is the chemical potential of species $i$; $\Delta q$ is the number of electrons removed to the reservoir (i.e., +1 for a singly positively charged defect and −1 for a singly negatively charged defect); and $\mu_F$ is the Fermi level. We calculate formation energies in the O-rich limit with the Fermi level equal to the valence-band maximum (VBM), assuming the dopant sources are molecular $P_4O_{10}$, solid cubic $As_2O_3$, and solid cubic $Sb_2O_3$. Finite-size scaling[23] was used to account for supercell-size effects.[24]

The defect transition level $\varepsilon(q,q')$ is defined as the Fermi level at which the $q$- and $q'$-charge states have equal formation energies and can be calculated as[22]

$$\varepsilon(q,q') = \frac{E_f(q) - E_f(q')}{q' - q}, \qquad (2)$$

 

using the values of $E_f$ calculated with $\mu_F$ equal to the VBM.

In searching for stable defect complexes in multicomponent alloys, dozens or even hundreds of configurations and multiple stable charge states may need to be considered. Due to the challenges of supercell-size convergence, accurate *ab initio* calculation of each configuration may require many days of calculation with even the fastest computing resources. This limitation means that comprehensive searches for defect-cluster structures are often impractical, and researchers must rely on intuition and qualitative arguments to identify the lowest energy configurations. Such approaches have guided several previous *ab initio* studies[1,25–28] which have focused on configurations of $D_{\mathrm{Zn}}$-$2\mathrm{V_{Zn}}$ complexes in which the $\mathrm{V_{Zn}}$ are separated from each other. The logic behind keeping the vacancies separated is that they tend to be negatively charged [with states $\mathrm{V_{Zn}}$ ($\mathrm{V^0_{Zn}}$, $\mathrm{V^{1-}_{Zn}}$, or $\mathrm{V^{2-}_{Zn}}$), depending on Fermi level] and will therefore likely repel each other. We checked this assumption by calculating the formation energy of neutral $\mathrm{As_{Zn}}$-$2\mathrm{V_{Zn}}$ starting with each of the 14 possible configurations with both $\mathrm{V_{Zn}}$ as first-nearest neighbors to $\mathrm{As_{Zn}}$. In neutral complexes, the individual vacancies that comprise the complex are centers of negative charge and the dopant a center of balancing positive charge. Consistent with the expected $\mathrm{V_{Zn}}$-$\mathrm{V_{Zn}}$ repulsion, we found that the mean formation energy of the six configurations with $\mathrm{V_{Zn}}$ 1NN to each other is 0.27 eV higher than the mean formation energy of configurations with $\mathrm{V_{Zn}}$ farther apart.[24]

Considering the $D_{\mathrm{Zn}}$-$2\mathrm{V_{Zn}}$ configurations with the most widely separated $\mathrm{V_{Zn}}$, Limpijumnong *et al.*[1] found that in several cases the formation energy was reduced when the dopant and an O shift so that the dopant is fivefold coordinated with O. They found that this occurred for the $q = 0$ and $-1$ charge states of $\mathrm{As_{Zn}}$-$2\mathrm{V_{Zn}}$ and all charge states of $\mathrm{Sb_{Zn}}$-$2\mathrm{V_{Zn}}$. We also found that the fivefold-coordinated Sb is more favorable; however, we found that this behavior is not present for As in large supercells. In small supercells it is relatively easy for shifting O to form a line defect which runs between images of the complex in the direction of the $c$ axis. In a large supercell, this line defect will not form, and the shift to fivefold coordination is 0.36 eV less favorable for the neutral complex. We found that P behaved similarly to As. We refer to these structures[24] as $D_{\mathrm{Zn}}$-$2\mathrm{V_{Zn}}$ in all that follows.

Despite the tendency for $\mathrm{V_{Zn}}$ to repel each other, we have found a set of highly stable configurations in which the $\mathrm{V_{Zn}}$ are 1NNs and the $D_{\mathrm{Zn}}$ moves off the lattice into an interstitial position between the $\mathrm{V_{Zn}}$. We refer to this cluster as a $D_I$-$3\mathrm{V_{Zn}}$ configuration. Similar interstitial-vacancy clusters have been found in other systems. In FeO and other binary oxides with the rock-salt-crystal structure,[29] tetrahedrally coordinated $M^{3+}$ cation interstitials are quite stable when surrounded by four cation vacancies. In $\mathrm{Cu_2O}$, Al and In impurities were found[30] to relax into voids formed by two $\mathrm{V_{Cu}}$'s, resulting in complexes similar to the ones we have calculated in ZnO.

When considering the stability of the $D_I$-$3\mathrm{V_{Zn}}$ configurations, it is helpful to think of the ZnO lattice as being composed of space-filling tetrahedra and octahedra with corner oxygens. For each Zn atom there is one filled tetrahedron, one empty tetrahedron, and one empty octahedron. If a cation is placed into a tetrahedral-interstitial position, it creates an occupied tetrahedron which shares one face and three edges with other cation-occupied tetrahedra. According to the Pauling rules,[31] this connectivity makes cation interstitials energetically unfavorable and therefore unlikely. However, if there are cation vacancies in place of the face-sharing tetrahedra, the interstitial position can in fact be quite stable for the dopant. This arrangement is what occurs in the stable configuration illustrated for As in Fig. 1(a), and we refer to it as $\mathrm{As_{tet}}$-$3\mathrm{V_{Zn}}$. There is a vacancy in the face-sharing tetrahedron and in two of the three edge-sharing tetrahedra around the As interstitial. As with the tetrahedral-interstitial position, the octahedral interstitial might also be expected to be unstable as it is both face sharing and edge sharing with three occupied tetrahedra. However, when the three face-sharing tetrahedra are unoccupied, it takes much less energy to fill the octahedral interstitial. This arrangement is illustrated for Sb in Fig. 1(b), and we refer to it as $\mathrm{Sb_{oct}}$-$3\mathrm{V_{Zn}}$. The calculated formation energies for $D_{\mathrm{Zn}}$-$2\mathrm{V_{Zn}}$ and $D_I$-$3\mathrm{V_{Zn}}$ defect clusters are plotted in Fig. 2 as a function of the Fermi level. The formation energies for the $q = 0$ and $-1$ charge states most relevant to $p$-type doping are listed in Table I along with the transition level $\varepsilon(0/-1)$, which in all that follows is given relative to the valence-band maximum.

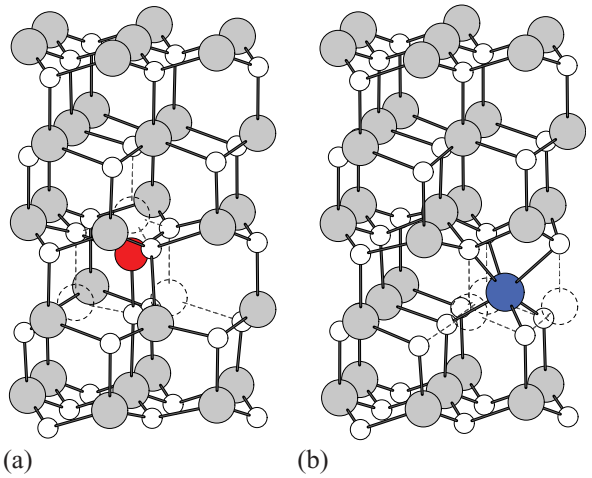


FIG. 1. (Color online) Configurations of the (a) neutral $\mathrm{As_{tet}}$-$3\mathrm{V_{Zn}}$ complex and (b) $\mathrm{Sb_{oct}}$-$3\mathrm{V_{Zn}}$ complex. Small white atoms are O, large gray atoms are Zn, red atoms are As, blue atoms are Sb, and dashed outlines indicate the $\mathrm{V_{Zn}}$ positions.

The relative stability of the $D_{\mathrm{Zn}}$-$2\mathrm{V_{Zn}}$ and $D_I$-$3\mathrm{V_{Zn}}$ complexes can be explained by considering Coulomb and strain energies. The $D_{\mathrm{tet}}$-$3\mathrm{V_{Zn}}$ complex is more stable than $D_{\mathrm{Zn}}$-$2\mathrm{V_{Zn}}$ in each case because of a decrease in Coulomb energy (due to the positively charged dopant being more closely bound to the negatively charged $\mathrm{V_{Zn}}$) without an increase in strain energy (because the cation-O distance is the same for substitutional- and tetrahedral-interstitial positions). In the $D_{\mathrm{oct}}$-$3\mathrm{V_{Zn}}$ configuration, the energy difference is strongly dependent on dopant size. The $\mathrm{P_{oct}}$-$3\mathrm{V_{Zn}}$ complex is very unstable, and the interstitial P shifts to one side to take on tetrahedral coordination.[24] The $\mathrm{As_{oct}}$-$3\mathrm{V_{Zn}}$ is unstable with an increase of $\sim$0.3 eV. However, $\mathrm{Sb_{oct}}$-$3\mathrm{V_{Zn}}$ is quite stable with an energy decrease of $\sim$1.2 eV. These trends can be explained by observing that the cation-O distance increases, moving from

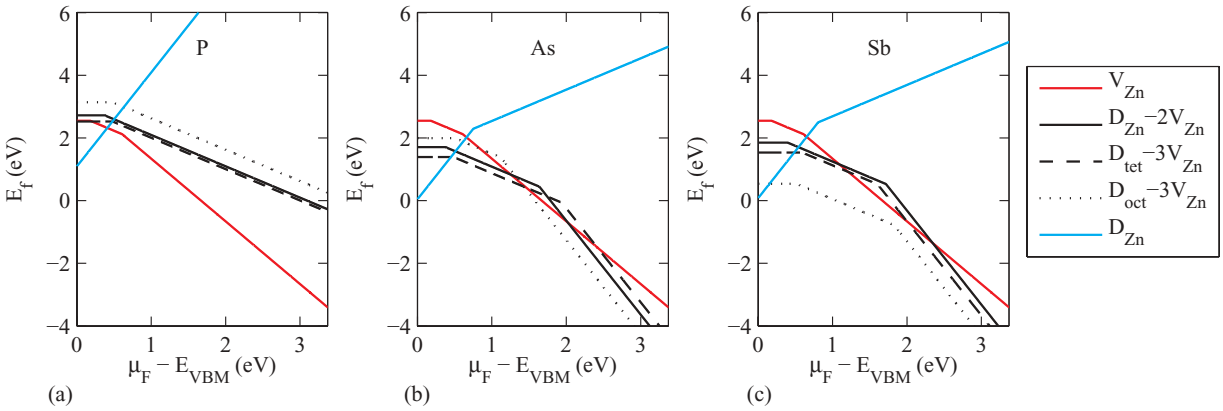


FIG. 2. (Color) GGA + U calculated formation energies as a function of the Fermi level for (a) P-, (b) As-, and (c) Sb-containing complexes. The slopes of the lines indicate the charge states, and the values of $\mu_F - E_{VBM}$ (at which the slope changes) indicate the transition levels between the charge states.

the substitutional position to the octahedral-interstitial position and makes the $D_{oct}$-$3V_{Zn}$ configuration favorable for large Sb and strongly unfavorable for small P. It is interesting to note that the most stable configuration changes from $As_{tet}$-$3V_{Zn}$ in the $q = 0$ and $-1$ charge states to $As_{oct}$-$3V_{Zn}$ in the $q = -3$ charge state (see Fig. 2) as the additional electrons increase the effective size of As.

For each dopant, the $\varepsilon(0/-1)$-transition level of the most stable complex configuration is significantly greater than the experimentally identified level at 0.1–0.2 eV that is most often attributed to these types of complexes. The $D_{tet}$-$3V_{Zn}$ complex is most stable for P and As, and the $\varepsilon(0/-1)$-transition levels are at 0.48 eV and 0.49 eV, respectively. For Sb, the $D_{oct}$-$3V_{Zn}$ complex is most stable, and the $\varepsilon(0/-1)$-transition level is 0.51 eV.

TABLE I. Formation energies and transition levels (measured in electronvolts) relative to the VBM for complexes in the $q = 0$ and $-1$ charge states, including values are for O-rich conditions with the Fermi level equal to the VBM. HSE calculations were performed in 108-atom supercells with Γ-only $k$-point sampling.

| Calculation Method | Complex | $E_f$ ($q = 0$) | $E_f$ ($q = -1$) | $\varepsilon(0/-1)$ |
|---|---|---|---|---|
| LDA[a] | $As_{Zn}$-$2V_{Zn}$ | 1.59 | 1.74 | 0.15 |
| | $Sb_{Zn}$-$2V_{Zn}$ | 2.00 | 2.16 | 0.16 |
| GGA | $P_{Zn}$-$2V_{Zn}$ | | | 0.12[b] |
| | | | | 0.18[c] |
| | $As_{Zn}$-$2V_{Zn}$ | 1.64 | 1.81 | 0.17 |
| | $Sb_{Zn}$-$2V_{Zn}$ | 1.78 | 1.93 | 0.16 |
| | $As_{tet}$-$3V_{Zn}$ | 1.45 | 1.72 | 0.28 |
| | $Sb_{oct}$-$3V_{Zn}$ | 0.80 | 1.09 | 0.28 |
| GGA + U | $P_{Zn}$-$2V_{Zn}$ | 2.72 | 3.10 | 0.37 |
| | $As_{Zn}$-$2V_{Zn}$ | 1.71 | 2.08 | 0.38 |
| | $Sb_{Zn}$-$2V_{Zn}$ | 1.85 | 2.25 | 0.40 |
| | $P_{tet}$-$3V_{Zn}$ | 2.52 | 3.01 | 0.48 |
| | $As_{tet}$-$3V_{Zn}$ | 1.39 | 1.88 | 0.49 |
| | $Sb_{tet}$-$3V_{Zn}$ | 1.53 | 2.13 | 0.60 |
| | $P_{oct}$-$3V_{Zn}$ | 3.14 | 3.63 | 0.49 |
| | $As_{oct}$-$3V_{Zn}$ | 1.99 | 2.50 | 0.50 |
| | $Sb_{oct}$-$3V_{Zn}$ | 0.54 | 1.05 | 0.51 |
| HSE | $As_{Zn}$-$2V_{Zn}$ | 3.18 | 4.47 | 1.28 |
| | $As_{tet}$-$3V_{Zn}$ | 2.82 | 4.47 | 1.65 |

[a]Reference 1.
[b]Reference 25.
[c]Reference 26.

The approximate treatment of correlation in the GGA + U leads to errors in band-gap and hole localization that can alter the $\varepsilon(0/-1)$-transition levels. To correct these errors, we performed select GGA and Heyd-Scuseria-Ernzerhof (HSE)[32] hybrid-Hartree-Fock density-functional calculations. Due to computational expense, the HSE calculations were performed in supercells with 108 atoms in the undefected cell with Γ-only $k$-point sampling. The HSE-screening parameter was 0.2 $Å^{-1}$, and the fraction of nonlocal Fock exchange was set to $a = 0.375$ to match the experimental band gap.[33] In terms of the band gap, the GGA + U correction increases the calculated band gap to 1.82 eV from 0.73 eV for GGA, and HSE calculations further increase the band gap to 3.43 eV, equivalent to the experimental value.

In addition to errors in the band gap, the GGA + U calculations do not properly localize holes on the oxygen atoms neighboring $V_{Zn}$.[22,34] We have found that this delocalization also occurs for the clusters. For the neutral $As_{Zn}$-$2V_{Zn}$ and $As_{tet}$-$3V_{Zn}$ clusters, GGA + U delocalizes the hole among the O that are neighboring $V_{Zn}$ but away from the dopant. In the HSE calculations, the hole is localized at one such O atom, and the system undergoes a corresponding Jahn-Teller distortion. Note that the $-1$ charged clusters do not have any holes, and therefore, localization is not an issue. We have not attempted to isolate the relative contributions of the band-gap correction and hole localization to the formation energy of the cluster. However, relative to the GGA + U calculations, the combined effects clearly move the acceptor state deeper into the band gap. Both the localized and delocalized holes have moments and raise the issue of the magnetic moments and how their coupling might impact our energies. For the hybrid calculations, we obtain primarily just one localized hole with a moment of nearly 1 $\mu_B$, so the only coupling of importance is that between clusters (intercluster interactions) in different image cells. However, magnetic interactions are typically quite short range, and due to the size of the periodic

supercells, we expect that intercluster magnetic coupling is negligible.[34] For the GGA + U calculations, we also expect weak intercluster magnetic coupling. However, as the moments occur on multiple oxygens, they can interact within a cluster (intracluster interactions). For the $As_{Zn}$-$2V_{Zn}$ cluster, the moments from Bader analysis show values less than 0.07 $\mu_B$ on all oxygens except three, which have moments of 0.16 $\mu_B$, 0.18 $\mu_B$, and 0.19 $\mu_B$. Thus, the intracluster ordering is effectively ferromagnetic. For the $As_{tet}$-$3V_{Zn}$ cluster there are four oxygens with significant moments, and they all have similar values of 0.16–0.17 $\mu_B$. Thus, the intracluster ordering for $As_{tet}$-$3V_{Zn}$ is ferromagnetic. We assume that these orderings are the lowest energy state and that, given the small values of the moments, the different magnetic orderings are similar in energy (which would likely lead to paramagnetic ordering at any reasonable temperature). A calculation of the ferrimagnetic ordering for $As_{Zn}$-$2V_{Zn}$ resulted in an energy change of less than 10 meV for the 254-atom cell.

The results of these hybrid studies, listed in Table I, confirm that $D_I$-$3V_{Zn}$ is the most stable complex configuration and has a deep acceptor level. The GGA calculations put the $D_{Zn}$-$2V_{Zn}$ $\varepsilon(0/-1)$-transition level at 0.17 eV and 0.16 eV for As and Sb complexes, respectively. This is in good agreement with previous local density approximation (LDA) calculations.[1] Also, in agreement with the trends in the GGA + U calculations, the $\varepsilon(0/-1)$-transition level in the more stable $D_I$-$3V_{Zn}$ complex is deeper than for the $D_{Zn}$-$2V_{Zn}$ complex with a value of 0.28 eV for both As and Sb complexes. The HSE calculations show that the $\varepsilon(0/-1)$-transition levels are deep at 1.28 eV for the $As_{Zn}$-$2V_{Zn}$ complex and 1.65 eV for the $As_{tet}$-$3V_{Zn}$ complex.

Along with the recent recalculation[35] of the $N_O$-acceptor level in ZnO which found that it is not shallow but deep in the band gap, these results highlight the importance of accounting for the LDA/GGA-band-gap problem in calculations of wide-band-gap semiconductors. Underestimating the defect levels also results in an underestimated formation energy since electrons occupying defect levels are at a lower energy relative to the Fermi level than they would be otherwise.[22] Table I shows that the formation energy of group-V dopant-vacancy complexes increased by 1.4–2.6 eV in the HSE calculations relative to GGA + U. This trend is qualitatively consistent with the difference between our GGA + U calculations in which the formation energy of a single neutral $V_{Zn}$ is 2.55 eV and hybrid-functional calculations which find the formation energy is ∼4 eV.[33] We expect a similar formation-energy correction for the P- and Sb-containing complexes. The high formation energies of the complexes and their deep transition levels are strong evidence that the acceptor often observed in experiments with ionization energy 0.1–0.2 eV is not due to dopant-vacancy complexes.

In summary, *ab initio* calculations with corrections of the LDA/GGA-band-gap problem show that $D_I$-$3V_{Zn}$ are the most stable group-V dopant-vacancy complexes in ZnO but are too deep and have too high formation energies to create highly *p*-type ZnO. Stable interstitial-vacancy complexes such as the $D_I$-$3V_{Zn}$ complexes we observe in ZnO have been found in other systems and should be considered in future studies of multisublattice systems.

We are thankful to Anderson Janotti and Chris Van de Walle for helpful discussions. We gratefully acknowledge support for this work from the Department of Energy through Grant No. DEFG02-08ER46547 and computational support from the National Science Foundation through TeraGrid resources provided by Texas Advanced Computing Center under Grant No. TG-DMR090023.

[1] S. Limpijumnong, S. B. Zhang, S.-H. Wei, and C. H. Park, Phys. Rev. Lett. **92**, 155504 (2004).
[2] D.-K. Hwang, H.-S. Kim, J.-H. Lim, J.-Y. Oh, J.-H. Yang, S.-J. Park, K.-K. Kim, D. C. Look, and Y. S. Park, Appl. Phys. Lett. **86**, 151917 (2005).
[3] F. X. Xiu, Z. Yang, L. J. Mandalapu, J. L. Liu, and W. P. Beyermann, Appl. Phys. Lett. **88**, 052106 (2006).
[4] A. Allenic, X. Q. Pan, Y. Che, Z. D. Hu, and B. Liu, Appl. Phys. Lett. **92**, 022107 (2008).
[5] D. C. Look, G. M. Renlund, R. H. Burgener, and J. R. Sizelove, Appl. Phys. Lett. **85**, 5269 (2004).
[6] Y. R. Ryu, T. S. Lee, and H. W. White, Appl. Phys. Lett. **83**, 87 (2003).
[7] C. Morhain, M. Teisseire, S. Vézian, F. Vigué, F. Raymond, P. Lorenzini, J. Guion, G. Neu, and J.-P. Faurie, Phys. Status Solidi B **229**, 881 (2002).
[8] W. Guo, A. Allenic, Y. B. Chen, X. Q. Pan, Y. Che, Z. D. Hu, and B. Liu, Appl. Phys. Lett. **90**, 242108 (2007).
[9] F. X. Xiu, Z. Yang, L. J. Mandalapu, D. T. Zhao, and J. L. Liu, Appl. Phys. Lett. **87**, 252102 (2005).
[10] X. H. Pan, W. Guo, Z. Z. Ye, B. Liu, Y. Che, H. P. He, and X. Q. Pan, J. Appl. Phys. **105**, 113516 (2009).
[11] U. Wahl, E. Rita, J. G. Correia, A. C. Marques, E. Alves, and J. C. Soares, Phys. Rev. Lett. **95**, 215503 (2005).
[12] U. Wahl, J. G. Correia, T. Mendonça, and S. Decoster, Appl. Phys. Lett. **94**, 261901 (2009).
[13] A. Krtschil, A. Dadgar, N. Oleynik, J. Bläsing, A. Diez, and A. Krost, Appl. Phys. Lett. **87**, 262105 (2005).
[14] M. Schirra, R. Schneider, A. Reiser, G. M. Prinz, M. Feneberg, J. Biskupek, U. Kaiser, C. E. Krill, K. Thonke, and R. Sauer, Phys. Rev. B **77**, 125215 (2008).
[15] B. Sieber, A. Addad, S. Szunerits, and R. Boukherroub, J. Phys. Chem. Lett. **1**, 3033 (2010).
[16] S. Limpijumnong, L. Gordon, M. Miao, A. Janotti, and C. G. Van de Walle, Appl. Phys. Lett. **97**, 072112 (2010).
[17] G. Kresse and J. Hafner, Phys. Rev. B **47**, 558 (1993); **49**, 14251 (1994); G. Kresse and J. Furthmüller, Comput. Mater. Sci. **6**, 15 (1996); Phys. Rev. B **54**, 11169 (1996); G. Kresse and D. Joubert, *ibid.* **59**, 1758 (1999).
[18] J. P. Perdew, K. Burke, and M. Ernzerhof, Phys. Rev. Lett. **77**, 3865 (1996). **78**, 1396 (1997).
[19] V. Anisimov, F. Aryasetiawan, and A. Lichtenstein, J. Phys.: Condens. Matter **9**, 767 (1997).
[20] P. Erhart, K. Albe, and A. Klein, Phys. Rev. B **73**, 205203 (2006).

[21]H. J. Monkhorst and J. D. Pack, Phys. Rev. B **13**, 5188 (1976).
[22]A. Janotti and C. G. Van de Walle, Phys. Rev. B **76**, 165202 (2007).
[23]C. W. M. Castleton, A. Höglund, and S. Mirbt, Modell. Simul. Mater. Sci. Eng. **17**, 084003 (2009).
[24]See Supplemental Material at http://link.aps.org/supplemental/10.1103/PhysRevB.85.195207 for details on finite-size scaling.
[25]R.-Y. Tian and Y.-J. Zhao, J. Appl. Phys. **106**, 043707 (2009).
[26]W.-J. Lee, J. Kang, and K. J. Chang, Phys. B (Amsterdam, Neth.) **376–377**, 699 (2006); Phys. Rev. B **73**, 024117 (2006).
[27]R. Qin, J. Zheng, J. Lu, L. Wang, L. Lai, G. Luo, J. Zhou, H. Li, Z. Gao, G. Li, and W. N. Mei, J. Phys. Chem. C **113**, 9541 (2009).
[28]Y. Shen, L. Mi, X. Xu, J. Wu, P. Wang, Z. Ying, and N. Xu, Solid State Commun. **148**, 301 (2008).
[29]S. Tomlinson, J. Phys. Chem. Solids **51**, 477 (1990).
[30]A. F. Wright and J. S. Nelson, J. Appl. Phys. **92**, 5849 (2002).
[31]L. Pauling, J. Am. Chem. Soc. **51**, 1010 (1929).
[32]J. Heyd, G. E. Scuseria, and M. Ernzerhof, J. Chem. Phys. **118**, 8207 (2003). **124**, 219906 (2006).
[33]F. Oba, A. Togo, I. Tanaka, J. Paier, and G. Kresse, Phys. Rev. B **77**, 245202 (2008).
[34]J. A. Chan, S. Lany, and A. Zunger, Phys. Rev. Lett. **103**, 016404 (2009).
[35]J. L. Lyons, A. Janotti, and C. G. Van de Walle, Appl. Phys. Lett. **95**, 252105 (2009).